

# Synthesis, Crystal Structures and Fluorescence Properties of Two $d^{10}$ Metal Coordination Polymers with Flexible Bis(benzimidazolyl)alkane Ligands

Jun-Wen Wang<sup>a</sup>, Guang-Hua Cui<sup>b</sup>, Li Qin<sup>b</sup>, and Shu-Lin Xiao<sup>b</sup>

<sup>a</sup> School of Chemical and Materials Science, Shanxi Normal University, Linfen, 041004, P. R. China

<sup>b</sup> College of Chemical Engineering, Hebei United University, Tangshan, 063009, P. R. China

Reprint requests to Prof. Guang-Hua Cui. E-mail: [tscghua@126.com](mailto:tscghua@126.com)

*Z. Naturforsch.* **2013**, 68b, 250–256 / DOI: 10.5560/ZNB.2013-2319

Received December 12, 2012

Two  $d^{10}$  metal coordination polymers with bis-benzimidazole ligands,  $[(\text{Ag}(\text{L}^1))\cdot\text{NO}_3\cdot 4\text{H}_2\text{O}]_n$  (**1**) and  $[\text{Cu}_2(\text{L}^2)(\text{CN})_2]_n$  (**2**) [ $\text{L}^1 = 1,4\text{-bis}(\text{benzimidazol-1-yl})\text{butane}$ ,  $\text{L}^2 = 1,4\text{-bis}(5,6\text{-dimethylbenzimidazol-1-yl})\text{butane}$ ] have been synthesized hydrothermally and characterized by elemental analysis, IR spectroscopy, thermogravimetric (TG) analysis and single-crystal X-ray diffraction. Compound **1** features a ribbon-like chain structure bridged by  $\text{L}^1$  ligands, and is ultimately extended into a 2D supramolecular network through two kinds of  $\pi$ - $\pi$  stacking interactions. Compound **2** displays a (6,3) wave-like layer in which  $[\text{Cu}_6(\mu\text{-CN})_6(\text{L}^2)_2]_n$  double chains are interconnected by pairs of  $\text{L}^2$  bridges. The fluorescence properties of the compounds in the solid state at room temperature were investigated.

**Key words:** Bis-benzimidazole, Crystal Structure, Fluorescence Properties, Supramolecular Network

## Introduction

The design and assembly of coordination polymers with novel structures and physical and chemical properties relevant to catalysis, adsorption, luminescence, nonlinear optics, and magnetism are of great interest [1–4]. To date, the rational and controllable synthesis of coordination networks and supramolecular architectures are still an intricate challenge in most cases. Several factors, such as preferred coordination geometry of the metals, the functionality, flexibility and symmetry of the organic ligands, and the template effects of structure-directing agents may affect the assembly of the complexes [5–7]. Usually, the design of the bridging ligand is a useful way of manipulating polymeric structures. Among various organic ligands, flexible bis(benzimidazole) derivatives, which can satisfy the coordination needs of the metal centers and consequently generate more robust and intricate networks, have attracted much attention and have been widely used as classical *N*-

based ligands. In our previous studies, we prepared a series of bis-benzimidazole-type bridging ligands, which exhibited the ability to join metal ions in a variety of inorganic-organic arrangements ranging from discrete assemblies to infinite molecular networks [8–11]. These structurally varying architectures provide fascinating insight into the design of solid-state materials. The efficient luminescence from certain Cu(I) and Ag(I) complexes has been the subject of intense studies, particularly within the context of assigning the optical transitions involved. So, we and other groups have focused on the synthesis and structural exploration of metal coordination polymers with flexible bis-benzimidazole ligands [9–19]. In the study presented here the self-assembly reactions were carried out under hydrothermal conditions to give complexes  $[(\text{Ag}(\text{L}^1))\cdot\text{NO}_3\cdot 4\text{H}_2\text{O}]_n$  (**1**) and  $[\text{Cu}_2(\text{L}^2)(\text{CN})_2]_n$  (**2**) ( $\text{L}^1 = 1,4\text{-bis}(\text{benzimidazol-1-yl})\text{butane}$ ,  $\text{L}^2 = 1,4\text{-bis}(5,6\text{-dimethylbenzimidazol-1-yl})\text{butane}$ ). The crystal structures and solid-state fluorescence properties of these compounds are reported.

## Results and Discussion

### Crystal structure of $[(\text{Ag}(\text{L}^1))\cdot\text{NO}_3\cdot 4\text{H}_2\text{O}]_n$ (**1**)

X-Ray diffraction analysis has indicated that **1** crystallizes in the monoclinic space group  $P2_1/c$ . The asymmetric unit consists of one Ag(I) ion, one  $\text{L}^1$  ligand, one uncoordinated nitrate anion and four water molecules. As shown in Fig. 1, the Ag(I) ion is linearly coordinated by two imidazole nitrogen atoms from two different  $\text{L}^1$  ligands with distances  $\text{Ag1}-\text{N2} = 2.117(3)$  and  $\text{Ag}-\text{N4A} = 2.121(3)$  Å (symmetry code A:  $x-1, -y+3/2, z-1/2$ ). The angle  $\text{N2}-\text{Ag1}-\text{N4A}$  is  $165.69(11)^\circ$ , and the dihedral angle between the mean planes of the benzimidazole rings is  $3.08^\circ$ .

In **1**,  $\text{L}^1$  is a bridging bis(monodentate) ligand and connects the silver atoms forming a zigzag chain, as shown in Fig. 1. The distance between two adjacent Ag(I) atoms is  $13.505(13)$  Å, and the  $\text{Ag}\cdots\text{Ag}\cdots\text{Ag}$  angle is  $146.73^\circ$ . Furthermore, the chains are connected into a 2D supramolecular network through two different kinds of face-to-face  $\pi$ - $\pi$  stacking interactions. One is between imidazole rings of adjacent chains with the interplanar separation being  $3.449$  Å (the centroid-centroid and slippage distances are  $3.701$  and  $1.341$  Å, respectively); another one is between imidazole and benzene rings of benzimidazole molecules

of adjacent chains with an interplanar separation of  $3.412$  Å (the centroid-centroid and slippage distances are  $3.576$  and  $1.071$  Å, respectively), as depicted in Fig. 1.

Complex **1** contains large, solvent-accessible voids of about  $232$  Å<sup>3</sup> comprising 21.3% of the unit cell volume. Such porous materials may be potential candidates for applications such as gas absorption or gas sensing.

### Synthesis, UV/Vis spectrum and crystal structure of $[\text{Cu}_2(\text{L}^2)(\text{CN})_2]_n$ (**2**)

The self-assembly reaction of  $\text{CuCl}_2$ , the bidentate nitrogen ligands and  $\text{K}_3[\text{Fe}(\text{CN})_6]$  by hydrothermal syntheses is an effective route for the preparation of cyanide-bridged copper(I) complexes [20], for which the latter provides the cyanide anions. Under high temperature and pressure, copper(II) is readily reduced by the cyanide anion originating from the iron-cyano complex to form stable copper(I) complexes and  $(\text{CN})_2$  [20]. The reaction between  $\text{Cu}^{2+}$  and (uncomplexed)  $\text{CN}^-$  at ambient conditions has been known for a long time and is a well-established laboratory procedure for the preparation of  $\text{CuCN}$ .

As is common for metal cyanide complexes, complex **2** is insoluble in water and common organic sol-

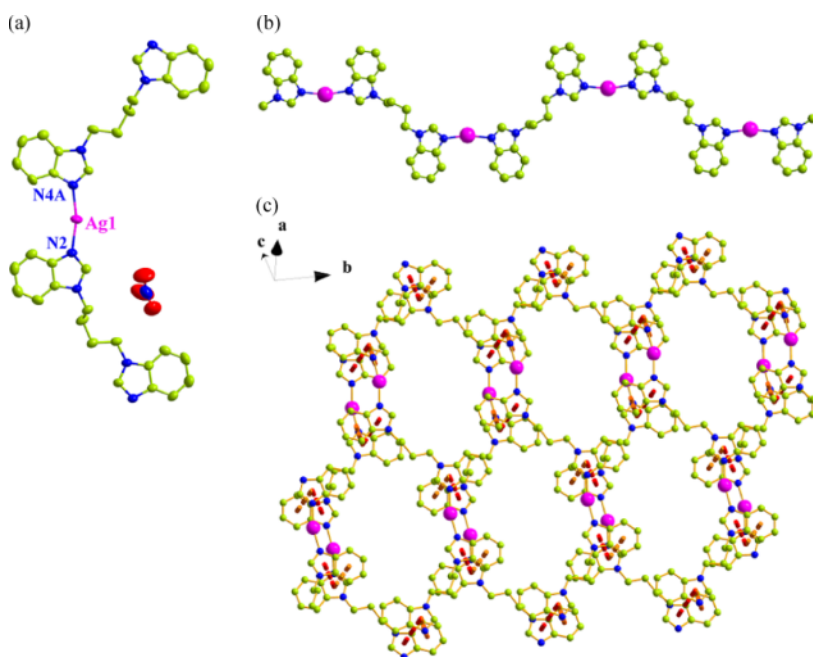


Fig. 1 (color online). a) Coordination environment of the Ag(I) atom in **1** with displacement ellipsoids drawn at the 30% probability level. Hydrogen atoms were omitted for clarity. Symmetry transformation used to generate equivalent atoms: A =  $x-1, -y+3/2, z-1/2$ ; b) the zig-zag chains formed by connecting  $\text{L}^1$  ligands in the crystal structure of **1**; c) the 2D supramolecular network formed by  $\pi$ - $\pi$  stacking interactions of **1** (some H atoms omitted for clarity).

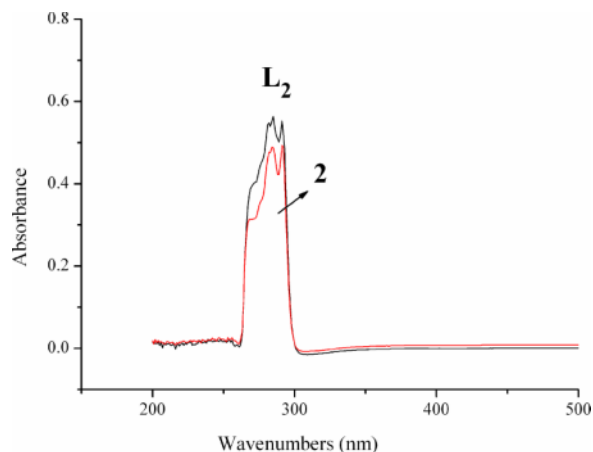


Fig. 2. The UV/Vis absorption spectra of ligand  $L^2$  and complex **2**.

vents such as methanol, ethanol, acetonitrile. The copper atom in **2** has the oxidation state +1 which can be inferred from the absence of color and the compo-

sition as ascertained by the crystal structure analysis. Furthermore, the UV/Vis absorption spectra of the ligands  $L^2$  and complex **2** in DMF solution were measured at room temperature (Fig. 2). The strong bands at 281, 285, 291 nm (for  $L^2$ ), and 285, 291 nm (for complex **2**) are ascribed to the  $\pi \rightarrow \pi^*$  transition within the benzimidazolyl rings.

The asymmetric unit of **2** contains two crystallographically independent copper(I) atoms, two  $CN^-$  anions, and one  $L^2$  ligand. As depicted in Fig. 3, compound **2** can be viewed as having zigzag  $[CuCN]_n$  chains, which are interconnected by pairs of  $L^2$  ligands to form a (6,3) layer.

Both Cu1 and Cu2 atoms are in trigonal-planar coordination geometries. As shown in Fig. 3, the Cu1 cation is bonded to three nitrogen atoms from one  $L^2$  ligand (Cu1–N5 = 2.037(3) Å) and two different  $CN^-$  anions (Cu1–N3 = 1.923(5) and Cu1–N4 = 1.928(5) Å). The bond angles range from 110.98(15) to 136.83(17)°; the Cu2 cation is ligated by two carbon atoms from two differ-

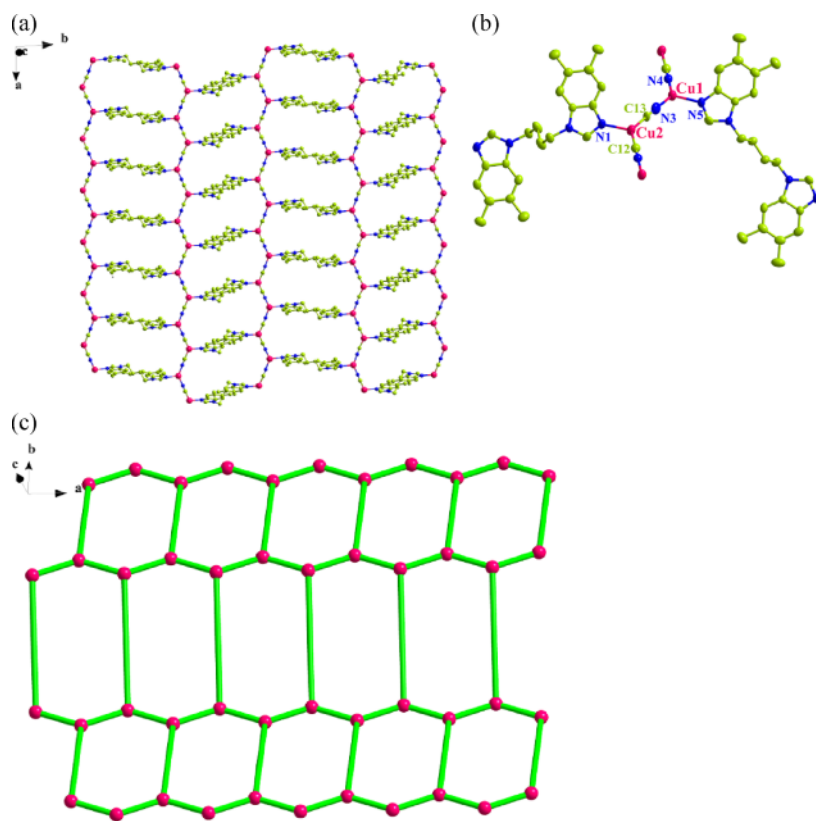


Fig. 3 (color online). a) The layer structure of **2** with  $L^2$  as connecting ligand; b) the coordination environment of the copper(I) atom in **2** with displacement ellipsoids drawn at the 30% probability level. The hydrogen atoms were omitted for clarity; c) the undulated (6,3) layers of complex **2**.

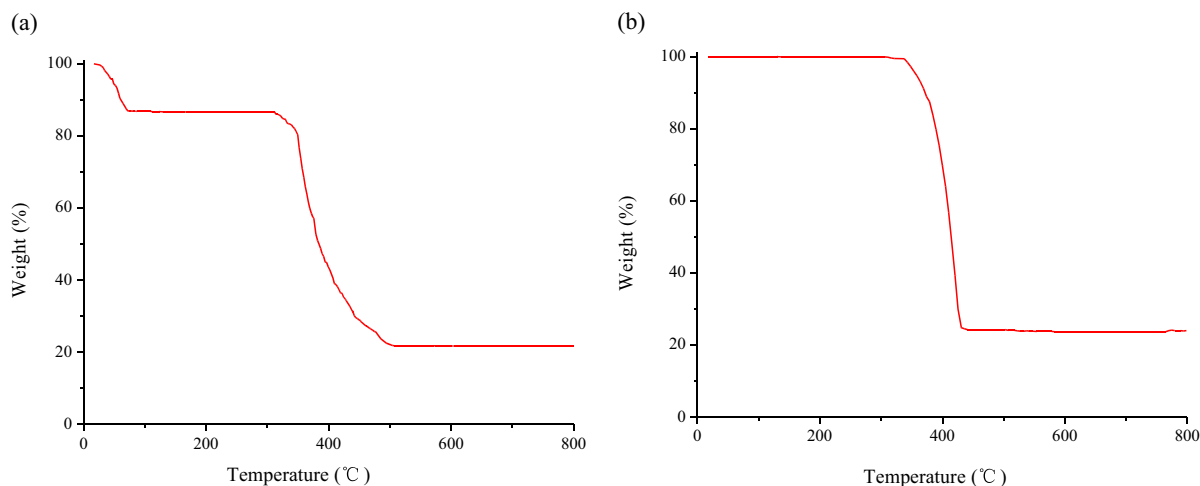


Fig. 4. a) TG curve of complex **1**; b) TG curve of complex **2**.

ent  $\text{CN}^-$  anions ( $\text{Cu2}-\text{C13} = 1.871(4)$  and  $\text{Cu2}-\text{C12} = 1.878(4)$  Å) and one nitrogen atom from one  $\text{L}^2$  ligand ( $\text{Cu2}-\text{N1} = 2.028(4)$  Å). The three coordination angles fall in the range of  $110.89(16)$  to  $136.23(18)^\circ$ .

Each  $\text{L}^2$  ligand exhibits a *trans-trans* configuration with the N-to-N distance of 5.368 Å (N2/N2B pair, symmetry code B:  $-x, -y - 1, -z + 2$ ) or 6.228 Å (N6/N6C pair, symmetry code C:  $-x + 1, -y + 2, -z + 2$ ), and the benzimidazolyl groups are parallel to each other. Topologically, each metallomacrocyclic unit is fused with its neighboring ones *via* sharing two  $\text{L}^2$  ligands to form a  $[\text{Cu}_6(\mu\text{-CN})_6(\text{L}^2)_2]_n$  double chain. Such a double chain is further interconnected by pairs of  $\text{L}^2$  bridges to form a 2D (6,3) network (Fig. 3). This undulated (6,3) net contains honeycomb-like cavities, separating two neighboring Cu atoms at distances of 4.946 (9) and 4.945 (8) Å.

#### IR spectroscopy

For compound **1**, the very strong and broad peak at  $3420\text{ cm}^{-1}$  arises from the OH stretching mode of water and the shoulder observed at  $1379\text{ cm}^{-1}$  is assigned to free nitrate ions. For compound **2** the band at  $2114\text{ cm}^{-1}$  is related to the bridging cyanide stretching vibration, which is consistent with the literature [20]. The strong bands at  $1615$  and  $1511\text{ cm}^{-1}$  for **1**, and at  $1622$  and  $1502\text{ cm}^{-1}$  for **2** can be assigned to vibrations of the benzimidazole rings.

#### Thermal analysis of complexes **1** and **2**

The thermal stability and thermal decomposition behavior of **1** and **2** were studied by thermal analysis in a static  $\text{N}_2$  atmosphere from room temperature to  $800^\circ\text{C}$ , as shown in Fig. 4. For compound **1**, the TG curve shows two steps of weight loss: the first one of 14% between  $26.7$  and  $69.2^\circ\text{C}$  corresponds to the removal of the four water molecules (calcd. 13.5%); the second one of 65% (calcd. 64.7%) takes place from  $311.0$  to  $495.5^\circ\text{C}$  and is assigned to the departure of the  $\text{L}^1$  ligand. The remaining residue of 22% is due to  $\text{Ag}_2\text{O}$  (calcd. 21.8%). The TG curve for compound **2** shows thermal stability up to  $337.1^\circ\text{C}$ . Afterwards continuous mass loss occurs in the temperature range from  $337.1$  to  $429.3^\circ\text{C}$  corresponding to the loss of all ligands. The remaining residual mass of 25% corresponds to the formation of Cu (calcd. 24.4%).

#### Fluorescence properties of compounds **1** and **2**

The photoluminescence properties of **1** and **2** and of the ligands of  $\text{L}^1$  and  $\text{L}^2$  in the solid state were studied at room temperature. The emission maxima are shown in Fig. 5. Upon excitation at 305 nm, complex **1** exhibits an emission maximum of middle intensity at 378 nm, which is shifted relative to that of the  $\text{L}^1$  ligand ( $\lambda_{\text{max}}^{\text{ex}} = 295\text{ nm}$ ,  $\lambda_{\text{max}}^{\text{em}} = 400\text{ nm}$ ). The bands might be assigned to intra-ligand ( $n \rightarrow \pi^*$  or  $\pi^* \rightarrow \pi^*$ ) transitions [21, 22]. Complex **2** shows an emission at 330 nm

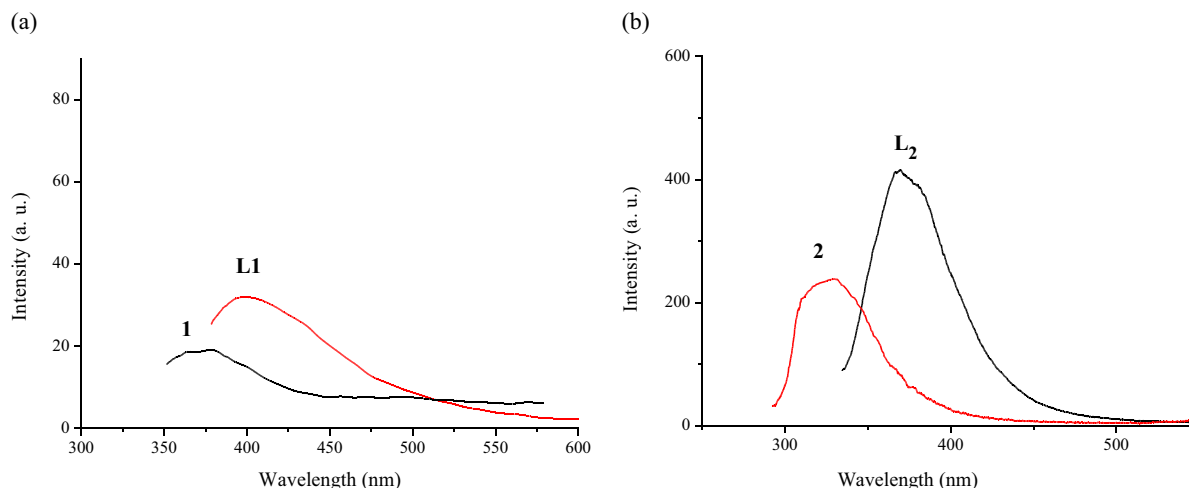


Fig. 5. a) Fluorescence emission spectra of  $L^1$  and complex **1**; b) fluorescence emission spectra of  $L^2$  and complex **2**.

upon excitation at 280 nm; compared with the free  $L^2$  ligand ( $\lambda_{\text{max}}^{\text{ex}} = 270$  nm,  $\lambda_{\text{max}}^{\text{em}} = 370$  nm), the emission is blue-shifted by 40 nm for **2**. The bands can be assigned as the metal-to-ligand charge transfer with electrons being transferred from the Cu(I) center to the unoccupied  $\pi^*$  orbitals of the cyanide groups [23, 24].

## Conclusion

Two  $d^{10}$  metal complexes based on flexible 1,4-bis(benzimidazol-1-yl)butane ligands have been synthesized hydrothermally. Structure analysis has shown that the anions and the supramolecular interactions determine the structures of this class of materials. Both complexes are fluorescent in the solid state.

## Experimental Section

### Materials and general methods

All the solvents and reagents for synthesis were commercially available and used as received. The  $L^1$  and  $L^2$  ligands were prepared according to literature procedures [25]. C, H, and N elemental analyses were performed on a Perkin Elmer 240 C analyzer. The IR spectra were recorded in the 4000–400  $\text{cm}^{-1}$  range using an FT-IR Avatar 360 (Nicolet) spectrophotometer with KBr pellets. The TG measurements were carried out on a Netzsch TG 209 thermal analyzer from room temperature to 800 °C under  $\text{N}_2$  with a heating rate of 10 °C  $\text{min}^{-1}$ . The fluorescence spectra were performed with a Hitachi F-7000 spectrophotometer at room temperature. UV/Vis spectra of **2** and the ligand  $L^2$  were obtained

with an Hitachi UV-3010 spectrophotometer in DMF solution ( $2.0 \times 10^{-5}$  mol  $\text{L}^{-1}$ ) at 298 K.

### Synthesis of $[(\text{Ag}(L^1))\cdot\text{NO}_3\cdot 4\text{H}_2\text{O}]_n$ (**1**)

**1** was synthesized by a one-pot hydrothermal reaction: the mixture of  $\text{AgNO}_3$  (0.2 mmol, 34 mg),  $L^1$  (0.2 mmol, 58 mg), and  $\text{H}_2\text{O}$  (12 mL) was sealed in a Teflon-lined autoclave and heated to 140 °C for 3 d under autogeneous pressure. Colorless block-shaped crystals of **1** were obtained after the autoclave was cooled to room temperature at a rate of 5 °C  $\text{h}^{-1}$ . Yield: ca. 43% based on  $\text{AgNO}_3$ . – Analysis for  $\text{C}_{18}\text{H}_{26}\text{AgN}_5\text{O}_7$  (532.30): calcd. C 40.6, H 4.9, N 13.1; found C 40.7, H 4.8, N 12.9%. – FTIR (KBr pellet,  $\text{cm}^{-1}$ ):  $\nu = 3420$  (vs), 3097 (w), 1615 (m), 1511 (m), 1379 (s), 1253 (w), 1185 (w), 741 (m).

### Synthesis of $[\text{Cu}_2(L^2)(\text{CN})_2]_n$ (**2**)

Compound **2** was prepared in a manner similar to that used for the preparation of **1**, but with  $\text{CuCl}_2\cdot 2\text{H}_2\text{O}$  (0.1 mmol, 17 mg),  $L^2$  (0.1 mmol, 35 mg),  $\text{K}_3\text{Fe}(\text{CN})_6$  (0.1 mmol, 32.9 mg), 10 mL of water and 5 mL of DMF (*N,N*-dimethylformamide). Yellow block-shaped crystals of **2** were obtained when the sample was cooled to room temperature at 5 °C  $\text{h}^{-1}$ . Yield: ca. 40% based on  $\text{CuCl}_2\cdot 2\text{H}_2\text{O}$ . – Analysis for  $\text{C}_{24}\text{H}_{26}\text{Cu}_2\text{N}_6$  (525.59): calcd. C 54.8, H 5.0, N 16.0; found C 54.9, H 4.9, N 15.9%. – FTIR (KBr pellet,  $\text{cm}^{-1}$ ):  $\nu = 3439$  (m), 2918 (w), 2114 (m), 1622 (w), 1502 (m), 1381 (m), 1067 (m), 469 (w).

### Crystal structure determinations

Single-crystal X-ray diffraction data of **1** and **2** were collected on a Bruker Smart 1000 CCD diffractome-

Table 1. Crystallographic data and details of data collection and structure refinement parameters of complexes **1** and **2**.

Compound	<b>1</b>	<b>2</b>
Empirical formula	C <sub>18</sub> H <sub>26</sub> AgN <sub>5</sub> O <sub>7</sub>	C <sub>24</sub> H <sub>26</sub> Cu <sub>2</sub> N <sub>6</sub>
Formula weight	532.30	525.59
Crystal size, mm <sup>3</sup>	0.16 × 0.15 × 0.12	0.13 × 0.12 × 0.12
Crystal system	monoclinic	monoclinic
Space group	<i>P</i> 2 <sub>1</sub> / <i>c</i>	<i>P</i> 2 <sub>1</sub> / <i>c</i>
<i>a</i> , Å	7.5423(9)	9.2129(6)
<i>b</i> , Å	11.7834(14)	9.5467(9)
<i>c</i> , Å	25.477(3)	27.605(3)
β, deg	105.611(3)	102.490(9)
<i>V</i> , Å <sup>3</sup>	2,180.7	2,370.5(4)
<i>Z</i>	4	4
<i>D</i> <sub>calcd.</sub> , g cm <sup>−3</sup>	1.40	1.47
μ (Mo <i>K</i> α), mm <sup>−1</sup>	0.9	1.8
<i>F</i> (000), e	928	1,080
<i>T</i> , K	293(2)	293(2)
<i>hkl</i> range	±9, −13 → 15, −33 → 26	−10 → 7, −11 → 7, ±32
Refl. measd. / unique /	12 962 / 4963 /	9379 / 4179 /
<i>R</i> <sub>int</sub>	0.0465	0.0413
GoF ( <i>F</i> <sup>2</sup> )	0.887	1.008
<i>R</i> 1 / <i>wR</i> 2 [ <i>I</i> > 2σ( <i>I</i> )]	0.0434 / 0.0920	0.0508 / 0.1025
<i>R</i> 1 / <i>wR</i> 2 (all data)	0.0868 / 0.1026	0.0962 / 0.1205
Δρ <sub>fin</sub> (max / min), e Å <sup>−3</sup>	0.45 / −0.37	0.48 / −0.26

ter with graphite-monochromatized Mo *K*α radiation (λ = 0.71073 Å) in ω–2θ scan mode at 293 K (Table 1). A semi-empirical absorption correction was applied using the program SADABS [26]. The structures were solved by Direct Methods and refined anisotropically by full-matrix least-squares technique using the program package SHELXTL [27, 28]. Metal atoms in each complex were located from the *E*-maps, and other non-hydrogen atoms were located in successive difference Fourier syntheses and refined with anisotropic displacement parameters on *F*<sup>2</sup>. The

Table 2. Selected bond lengths (Å) and angles (deg) for complexes **1** and **2**.

Complex <b>1</b> <sup>a</sup>			
Ag1–N2	2.117(3)	Ag1–N4A	2.121(3)
N2–Ag1–N4A	107.6(3)		
Complex <b>2</b>			
Cu1–N3	1.923(5)	Cu1–N4	1.928(5)
Cu1–N5	2.037(3)	Cu2–C13	1.871(4)
Cu2–C12	1.878(4)	Cu2–N1	2.028(4)
N3–Cu1–N4	136.83(17)	N3–Cu1–N5	110.98(15)
N4–Cu1–N5	112.08(15)	C13–Cu2–C12	136.23(18)
C13–Cu2–N1	112.88(16)	C12–Cu2–N1	110.89(16)

<sup>a</sup> Symmetry transformations used to generate equivalent atoms: *x* – 1, –*y* + 3/2, *z* – 1/2.

hydrogen atoms of the organic ligands were generated geometrically and refined in a riding model with isotropic displacement parameters. In the structure of **1**, the four water molecules were found to be severely disordered. Their electron density was removed from the diffraction intensities with the routine SQUEEZE of the program PLATON [28, 29] PLATON was also used for the evaluation of the structure determinations and some the geometry calculations. Selected bond lengths and angles of **1** and **2** are listed in Table 2.

CCDC 912885 and 912886 contain the supplementary crystallographic data for this paper. These data can be obtained free of charge from The Cambridge Crystallographic Data Centre via [www.ccdc.cam.ac.uk/data-muderscorequest/cif](http://www.ccdc.cam.ac.uk/data-muderscorequest/cif).

#### Acknowledgement

This work was supported by the National Natural Science Foundation of Shanxi Province of China (no. 2011011006-4) and the Foundation of Shan'xi Educational Committee (no. 20101111).

- [1] B. Xiao, L. J. Yang, H. Y. Xiao, S. M. Fang, *J. Coord. Chem.* **2011**, 64, 4408.
- [2] S. L. Xiao, X. Du, L. Qin, C. H. He, G. H. Cui, *J. Inorg. Organomet. Polym.* **2012**, 22, 1384.
- [3] H. X. Yang, X. R. Meng, Y. Liu, H. W. Hou, Y. T. Fan, X. Q. Shen, *J. Solid. State. Chem.* **2008**, 181, 2178.
- [4] G. H. Cui, C. H. He, C. H. Jiao, J. C. Geng, V. A. Blatov, *CrystEngComm* **2012**, 14, 4210.
- [5] J. Lee, O. K. Farha, J. Roberts, K. A. Scheidt, S. T. Nguyen, J. T. Hupp, *Chem. Soc. Rev.* **2009**, 38, 1450.
- [6] J. C. Geng, L. Qin, C. H. He, G. H. Cui, *Transition Met. Chem.* **2012**, 37, 579.
- [7] X. L. Wang, S. Yang, G. C. Liu, L. L. Hou, H. Y. Lin, A. X. Tian, *Transition Met. Chem.* **2011**, 36, 891.
- [8] C. H. Jiao, C. H. He, J. C. Geng, G. H. Cui, *Transition Met. Chem.* **2012**, 37, 17.
- [9] G. H. Cui, J. R. Li, J. L. Tian, X. H. Bu, S. R. Batten, *Cryst. Growth Des.* **2005**, 5, 1775.
- [10] T. F. Liu, W. F. Wu, W. G. Zhang, G. H. Cui, *Z. Anorg. Allg. Chem.* **2011**, 637, 148.
- [11] S. L. Xiao, Y. Q. Zhao, C. H. He, G. H. Cui, *J. Coord. Chem.* **2013**, 66, 89.
- [12] L. Hou, W. J. Shi, Y. Y. Wang, H. H. Wang, L. Cui, P. X. Chen, Q. Z. Shi, *Inorg. Chem.* **2011**, 50, 261.
- [13] L. L. Li, L. L. Liu, A. X. Zheng, Y. J. Chang, M. Dai, Z. G. Ren, H. X. Li, J. P. Lang, *Dalton Trans.* **2010**, 39, 7659.

- [14] J. L. Du, T. L. Hu, S. M. Zhang, Y. F. Zeng, X. H. Bu, *CrystEngComm* **2008**, *10*, 1866.
- [15] M. D. Allendorf, C. A. Bauer, R. K. Bhakta, R. J. T. Houk, *Chem. Soc. Rev.* **2009**, *38*, 1330.
- [16] J. P. Zhang, S. Kitagawa, *J. Am. Chem. Soc.* **2008**, *130*, 907.
- [17] F. M. Sarkar, K. Biradha, *Chem. Commun.* **2005**, 2229.
- [18] B. Xiao, W. Li, H. W. Hou, Y. T. Fan, *J. Coord. Chem.* **2009**, *62*, 1630.
- [19] H. Q. Hao, W. T. Liu, W. Tan, Z. J. Lin, M. L. Tong, *Cryst. Growth Des.* **2009**, *9*, 457.
- [20] Y. N. Chi, F. Y. Cui, Y. Q. Xu, C. W. Hu, *Eur. J. Inorg. Chem.* **2007**, *27*, 4375.
- [21] Y. B. Dong, H. Y. Wang, J. P. Ma, D. Z. Shen, R. Q. Huang, *Inorg. Chem.* **2005**, *44*, 4679.
- [22] X. L. Wang, S. Yang, G. C. Liu, J. X. Zhang, H. Y. Lin, A. X. Tian, *Inorg. Chim. Acta* **2011**, *375*, 70.
- [23] V. W. Yam, K. K. Lo, *Chem. Soc. Rev.* **1999**, *28*, 323.
- [24] A. Horváth, C. E. Wood, *Inorg. Chem.* **1994**, *33*, 5351.
- [25] X. J. Xie, G. S. Yang, L. Cheng, F. Wang, *Hua xue Shi ji* **2000**, *22*, 222.
- [26] G. M. Sheldrick, SADABS (version 2.03), Program for Empirical Absorption Correction of Area Detector Data, University of Göttingen, Göttingen (Germany) **2002**.
- [27] G. M. Sheldrick, *Acta Crystallogr.* **2008**, *A64*, 112.
- [28] A. L. Spek, PLATON, A Multipurpose Crystallographic Tool, Utrecht University, Utrecht (The Netherlands) **2010**.
- [29] A. L. Spek, *J. Appl. Crystallogr.* **2009**, *D65*, 148.